

LiDAR Technologies and Systems

Paul McManamon

SPIE PRESS

Bellingham, Washington USA

Library of Congress Cataloging-in-Publication Data

Names: McManamon, Paul F., 1946– author.

Title: LiDAR technologies and systems / Paul McManamon.

Description: Bellingham, Washington, USA : SPIE Press, [2019] | Includes bibliographical references and index.

Identifiers: LCCN 2018053788 | ISBN 9781510625396 (hard cover ; alk. paper) | ISBN 1510625399 (hard cover ; alk. paper) | ISBN 9781510625402 (PDF) | ISBN 1510625402 (PDF) | ISBN 9781510625419 (ePub) | ISBN 1510625410 (ePub) | ISBN 9781510625426 (Kindle/Mobi) | ISBN 1510625429 (Kindle/Mobi)

Subjects: LCSH: Optical radar.

Classification: LCC TK6592.O6 M36 2019 | DDC 621.3848–dc23

LC record available at <https://lccn.loc.gov/2018053788>

Published by

SPIE

P.O. Box 10

Bellingham, Washington 98227-0010 USA

Phone: +1 360.676.3290

Fax: +1 360.647.1445

Email: books@spie.org

Web: <http://spie.org>

Copyright © 2019 Society of Photo-Optical Instrumentation Engineers (SPIE)

All rights reserved. No part of this publication may be reproduced or distributed in any form or by any means without written permission of the publisher.

The content of this book reflects the work and thought of the author. Every effort has been made to publish reliable and accurate information herein, but the publisher is not responsible for the validity of the information or for any outcomes resulting from reliance thereon.

Cover imagery collected by Lincoln lidar sensor and provided by the Active Optical Systems Group, MIT Lincoln Laboratory.

Printed in the United States of America.

First Printing.

For updates to this book, visit <http://spie.org> and type “PM300” in the search field.

SPIE.

Contents

<i>Preface</i>	<i>xiii</i>
1 Introduction to LiDAR	1
1.1 Context of LiDAR	1
1.2 Conceptual Discussion of LiDAR	5
1.3 Terms for Active EO Sensing	6
1.4 Types of LiDARs	8
1.4.1 Some LiDARs for surface-scattering (hard) targets	10
1.4.2 Some LiDARs for volume-scattering (soft) targets	11
1.5 LiDAR Detection Modes	11
1.6 Flash LiDAR versus Scanning LiDAR	13
1.7 Eye Safety Considerations	14
1.8 Laser Safety Categories	16
1.9 Monostatic versus Bistatic LiDAR	17
1.10 Transmit/Receive Isolation	18
1.11 Major Devices in a LiDAR	18
1.11.1 Laser sources	18
1.11.2 Receivers	19
1.11.3 Apertures	19
1.12 Organization of the Book	20
Problems and Solutions	20
References	27
2 History of LiDAR	29
2.1 Rangefinders, Altimeters, and Designators	30
2.1.1 First steps of rangefinders	30
2.1.2 Long-distance rangefinders	32
2.1.3 Laser altimeters	34
2.1.4 Laser designators	35
2.1.5 Obstacle avoidance applications	36
2.2 Early Coherent LiDARs	38
2.2.1 Early work at MIT/Lincoln Lab	38
2.2.2 Early coherent LiDAR airborne applications	38
2.2.3 Autonomous navigation using coherent LiDAR	41

2.2.4	Atmospheric wind sensing	43
2.2.4.1	Early coherent LiDAR wind sensing	43
2.2.4.2	Early noncoherent wind measurement	46
2.2.5	Laser vibrometry	48
2.2.6	Synthetic-aperture LiDAR	50
2.3	Early Space-based LiDAR	51
2.4	Flight-based Laser Vibrometers	55
2.5	Environmental LiDARs	56
2.5.1	Early steps	56
2.5.2	Multiwavelength LiDARs	57
2.5.3	LiDAR sensing in China	57
2.5.4	LiDAR sensing in Japan	59
2.6	Imaging LiDARs	61
2.6.1	Early LiDAR imaging	61
2.6.2	Imaging LiDARs for manufacturing	63
2.6.3	Range-gated imaging programs	64
2.6.4	3D LiDARs	65
2.6.5	Imaging for weapon guidance	66
2.6.6	Flash-imaging LiDARs	67
2.6.7	Mapping LiDARs	68
2.6.7.1	Terrain mapping	68
2.6.8	LiDARs for underwater: Laser-based bathymetry	70
2.6.9	Laser micro-radar	71
2.6.9.1	Optical coherence tomography	71
2.6.9.2	Wavefront sensing	72
2.7	History Conclusion	74
	References	76
3	LiDAR Range Equation	89
3.1	Introduction to the LiDAR Range Equation	89
3.2	Illuminator Beam	89
3.3	LiDAR Cross-Section	92
3.3.1	Cross-section of a corner cube	95
3.4	Link Budget Range Equation	96
3.5	Atmospheric Effects	99
3.5.1	Atmospheric scattering	101
3.5.2	Atmospheric turbulence	102
3.5.3	Aero-optical effects on LiDAR	103
3.5.4	Extended (deep) turbulence	103
3.5.5	Speckle	104
	Problems and Solutions	105
	Notes and References	112

4	Types of LiDAR	113
4.1	Direct-Detection LiDAR	113
4.1.1	1D range-only LiDAR	113
4.1.2	Tomographic imaging LiDAR	114
4.1.3	Range-gated active imaging (2D LiDAR)	116
4.1.4	3D scanning LiDAR	117
4.1.5	3D flash imaging	119
4.1.6	3D mapping applications	120
4.1.6.1	GNSS position data collection	121
4.1.6.2	Ground surveys	121
4.1.6.3	Data acquisition conditions	122
4.1.6.4	Data processing and dissemination	123
4.1.7	Laser-induced breakdown spectroscopy	136
4.1.8	Laser-induced fluorescence	136
4.1.9	Active multispectral LiDAR	137
4.1.10	LiDARs using polarization as a discriminant	139
4.2	Coherent LiDAR	140
4.2.1	Laser vibration detection	140
4.2.2	Range-Doppler imaging LiDAR	142
4.2.3	Speckle imaging LiDAR	143
4.2.4	Aperture-synthesis-based LiDAR	144
4.2.4.1	Synthetic-aperture LiDAR (SAL)	146
4.2.4.2	Inverse SAL	149
4.3	Multiple-Input, Multiple-Output Active EO Sensing	150
	Appendix 4.1: MATLAB [®] program showing synthetic-aperture pupil planes and MTFs	160
	Problems and Solutions	172
	References	178
5	LiDAR Sources and Modulations	181
5.1	Laser Background Discussion	181
5.2	Laser Waveforms for LiDAR	184
5.2.1	Introduction	184
5.2.2	High time-bandwidth product waveforms	186
5.2.2.1	Polypulse waveforms	187
5.2.2.2	Linear frequency modulation	187
5.2.2.3	Pseudo-random-coded LiDAR	188
5.2.3	Radiofrequency modulation of a direct-detection LiDAR	189
5.2.4	Femtosecond-pulse modulation LiDAR	190
5.2.5	Laser resonators	191
5.2.6	Three-level and four-level lasers	192
5.2.7	Laser-pumping considerations	194
5.2.8	Q-switched lasers for LiDAR	194

5.2.8.1	Pockels cells	195
5.2.9	Mode-locked lasers for LiDAR	196
5.2.10	Laser seeding for LiDAR	199
5.2.11	Laser amplifiers for LiDAR	200
5.3	Lasers Used in LiDAR	202
5.3.1	Diode lasers for LiDAR	203
5.3.1.1	Interband, edge-emitting diode lasers	203
5.3.1.2	Interband, vertical-cavity diode lasers	207
5.3.1.3	Quantum cascade lasers	208
5.3.1.4	Interband cascade lasers	210
5.4	Bulk Solid State Lasers for LiDAR	210
5.4.1	Fiber lasers for LiDAR	211
5.4.1.1	Higher-peak-power waveguide lasers for LiDAR	212
5.4.2	Nonlinear devices to change the LiDAR wavelength	212
5.4.2.1	Harmonic generation and related processes	214
5.4.2.2	Optical parametric generation	218
5.5	Fiber Format	221
	Problems and Solutions	227
	References	232
6	LiDAR Receivers	235
6.1	Introduction to LiDAR Receivers	235
6.2	LiDAR Signal-to-Noise Ratio	237
6.2.1	Noise probability density functions	238
6.2.2	Thermal noise	240
6.2.3	Shot noise	241
6.2.4	Background noise	242
6.2.4.1	Spectral filter technology	243
6.2.4.2	Calculation of background from solar flux	244
6.2.5	Dark current, $1/f$ noise, and excess noise	248
6.3	Avalanche Photodiodes and Direct Detection	248
6.3.1	Linear-mode APD arrays for LiDAR	251
6.3.1.1	InGaAs LMAPD arrays	252
6.3.1.2	HgCdTe LMAPD cameras	265
6.3.1.3	Summary of the advantages and disadvantages of LMAPDs for direct detection	268
6.3.2	Direct-detection GMAPD LiDAR camera	268
6.3.2.1	The effect of a bright sun background on GMAPDs	273
6.3.2.2	Coincidence processing for detection	274
6.3.2.3	Summary of the advantages and disadvantages of GMAPDs for direct detection	278
6.4	Silicon Detectors	279
6.5	Heterodyne Detection	280
6.5.1	Temporal heterodyne detection	281

6.5.2	Heterodyne mixing efficiency	282
6.5.3	Quadrature detection	283
6.5.4	Carrier-to-noise ratio (CNR) for temporal heterodyne detection	285
6.5.5	Spatial heterodyne detection / digital holography	285
6.5.5.1	SNR for spatial heterodyne detection	286
6.5.6	Receivers for coherent LiDARs	287
6.5.6.1	Acousto-optic frequency shifting	287
6.5.7	Geiger-mode APDs for coherent imaging	289
6.5.8	A p–i–n diode or LMAPD for coherent imaging	291
6.5.9	Sampling associated with temporal heterodyne sensing	292
6.6	Long–Frame–Time Framing Detectors for LiDAR	292
6.7	Ghost LiDARs	293
6.8	LiDAR Image Stabilization	294
6.9	Optical–Time-of-Flight Flash LiDAR	295
6.9.1	Summary of the advantages and disadvantages of OTOF cameras	297
	Problems and Solutions	298
	Notes and References	307
7	LiDAR Beam Steering and Optics	311
7.1	Mechanical Beam-Steering Approaches for LiDAR	311
7.1.1	Gimbals	311
7.1.2	Fast-steering mirrors	313
7.1.3	Risley prisms and Risley gratings	315
7.1.4	Rotating polygonal mirrors	318
7.1.5	MEMS beam steering for LiDAR	320
7.1.6	Lenslet-based beam steering	324
7.1.6.1	All-convex-lens–based steering	324
7.1.6.2	Mixed-lenslet arrays	325
7.2	Nonmechanical Beam-Steering Approaches for Steering LiDAR	
	Optical Beams	326
7.2.1	OPD-based nonmechanical approaches	327
7.2.1.1	Modulo 2π beam steering	327
7.2.1.2	Finest pointing angle	330
7.2.1.3	Largest steering angle for an OPA	331
7.2.1.4	Liquid crystal OPAs	332
7.2.1.5	Liquid crystal fringing field effect on steering efficiency	334
7.2.1.6	Quantization-caused reduction in steering efficiency	335
7.2.1.7	Steerable electro-evanescent optical refraction	336
7.2.1.8	Ferroelectric-SmC*–based beam steering	337
7.2.2	Chip-scale optical phased arrays	338
7.2.3	Electrowetting beam steering for LiDAR	338

7.2.4	Using electronically written lenslets for lenslet-based beam steering	339
7.2.5	Beam steering using EO effects	340
7.2.5.1	Prism-shaped-OPD-based beam steering	341
7.2.5.2	Space-charge-injection-mode KTN beam steering	353
7.2.5.3	Analysis of EO-crystal-film-based beam steering	363
7.2.6	Phased-based nonmechanical beam steering	364
7.2.6.1	Polarization birefringent grating beam steering	364
7.3	Some Optical Design Considerations for LiDAR	368
7.3.1	Geometrical optics	368
7.3.2	Adaptive optics systems	369
7.3.3	Adaptive optical elements	370
	Problems and Solutions	370
	Notes and References	378
8	LiDAR Processing	383
8.1	Introduction	383
8.2	Generating LiDAR Images/Information	383
8.2.1	Range measurement processing	383
8.2.2	Range resolution of LiDAR	384
8.2.2.1	Nyquist sampling a range profile	385
8.2.2.2	Unambiguous range	386
8.2.2.3	Threshold, leading edge, and peak detectors	387
8.2.2.4	Range accuracy, range precision, and range resolution	388
8.2.3	Angle LiDAR processing	389
8.2.3.1	Point spread function	389
8.2.3.2	Microscanning of LiDAR images for improved sampling	390
8.2.3.3	Multiple-subaperture spatial heterodyne processing	391
8.2.4	Gathering information from a temporally coherent LiDAR	392
8.2.4.1	Velocity resolution of LiDAR	393
8.2.4.2	Processing laser vibrometry data	394
8.2.5	General LiDAR Processing	396
8.2.5.1	Definitions of various LiDAR processing steps for geospatial images	396
8.2.5.2	Inertial measurement units	396
8.2.5.3	Data product types	397
8.2.5.4	Grayscale calculations	397
8.2.5.5	Fourier transforms	399
8.2.5.6	Developing 3D maps from LiDAR	400
8.2.6	Target classification using LiDAR	401
	Problems and Solutions	402
	References	408

9	Figures of Merit, Testing, and Calibration for LiDAR	409
9.1	Introduction	409
9.2	LiDAR Characterization and Figures of Merit	409
9.2.1	Ideal point response mainlobe width	410
9.2.2	Integrated sidelobe ratio	411
9.2.3	Peak sidelobe ratio	411
9.2.4	Spurious sidelobe ratio	411
9.2.5	Noise-equivalent vibration velocity	411
9.2.6	Abiguity velocity	412
9.2.7	Unambiguous range	412
9.3	LiDAR Testing	412
9.3.1	Angle/angle/range resolution testing	412
9.3.2	Velocity measurement	414
9.3.3	Measuring range walk	415
9.4	LiDAR Calibration	416
9.4.1	Dark nonuniformity correction	419
9.4.2	Results of correction	421
	Problems and Solutions	424
	References	425
10	LiDAR Performance Metrics	427
10.1	Image Quality Metrics	427
10.1.1	Object parameters	428
10.1.1.1	Additional object characteristics	432
10.2	LiDAR Parameters	433
10.3	Image Parameters: National Imagery Interpretability Rating Scale (NIIRS)	433
10.4	3D Metrics for LiDAR Images	437
10.5	General Image Quality Equations	437
10.6	Quality Metrics Associated with Automatic Target Detection, Recognition, or Identification	439
10.7	Information Theory Related to Image Quality Metrics	440
10.8	Image Quality Metrics Based on Alternative Basis Sets	441
10.9	Eigenmodes	441
10.10	Compressive Sensing	442
10.10.1	Knowledge-enhanced compressive sensing	442
10.10.2	Scale-invariant feature transforms	442
10.11	Machine Learning	443
10.12	Processing to Obtain Imagery	443
10.13	Range Resolution in EO/IR Imagers	444
10.14	Current LiDAR Metric Standards	445
10.15	Conclusion	445
	Appendix 10-1 MATLAB code to Fourier transform an image	445

Problems and Solutions	446
References	455
11 Significant Applications of LiDAR	459
11.1 Auto LiDAR	459
11.1.1 Introduction	459
11.1.2 Resolution	460
11.1.3 Frame rate	462
11.1.4 Laser options	464
11.1.5 Eye safety	464
11.1.6 Unambiguous range	465
11.1.7 Required laser energy per pulse and repetition rate	465
11.1.8 Obscurants considered for auto LiDAR	470
11.1.9 Keeping the auto LiDAR aperture clear	470
11.2 3D Mapping LiDAR	471
11.2.1 Introduction to 3D mapping LiDAR	471
11.2.2 3D Mapping LiDAR design	477
11.3 Laser Vibrometers	477
11.3.1 Designing a laser vibrometer	480
11.4 Wind Sensing	481
Problems and Solutions	483
References	496
<i>Index</i>	499

Preface

About six years ago, I co-taught a semester-long course in LiDAR technology with Dr. Ed Watson at the LiDAR and Optical Communications Institute (LOCI) of the University of Dayton. At the time, there was a book that covered part of what I wanted to teach, but it did not cover all of the areas I thought should go into the course. There were a couple of other books that had interesting LiDAR-related material, but no book that covered all of the topics that I thought were needed. Since then, I have done a number of week-long, or almost-week-long, courses. One of those I co-taught with Gary Kamerman, and a number of them with Ed Watson. Shortly after teaching that 2012 semester-long course, I started writing the *Field Guide to LiDAR*, which was published by SPIE Press in 2015. I thought a shorter book would be easier to write than a longer one. I was wrong. The Field Guide came out great, but its format with one topic per page made it a challenging type of book to write. Also, when I finished writing the Field Guide, I still did not have a really good *text* book on LiDAR technology and systems. Thus, the decision to write this book grew out of the need for a good teaching reference for a longer course on LiDAR. The Field Guide is great as a quick reference, with all the equations in one place and each topic concisely presented, but it does not provide enough background or detail to be a text book. This book presents an in-depth coverage of LiDAR technology and systems, and the Field Guide serves as a reminder of the essential points and equations once you already understand the technology.

I learned a lot writing the *Field Guide to LiDAR*, and then writing this book. When I considered all of the topics that should be covered in this book, there were some I knew really well, and some I knew less well. The neat thing I found about writing a book like this is that, before I could effectively explain a particular concept, I needed to clearly understand the concept. To this end, the comparison paper I recently wrote¹ with Ed Watson, Andrew Huntington, Dale Fried, Paul Banks, and Jeffrey D. Beck taught me a lot about receivers. I have included sections from that paper in this book. The paper on the history of laser radar in the U.S.² that I wrote with Milt Huffacker and Gary Kammerman, and the more recent paper³ “Laser radar: historical perspective—from the East to the West,” which I wrote with Vasly Molebny, Ove Steinvall, T. Kobayashi, and W. Chen, both provide a good summary of the history of LiDAR. Chairing the 2014 United States National

Academy of Sciences study on laser radar⁴ helped me learn more. Of course, decades of experience monitoring LiDAR development for the Air Force taught me a lot as well.

Once I started working on this book, I had two students take a self-study course with me in LiDAR. Both students read early versions of the manuscript and developed possible problems to include at the end of each chapters. Dr. Abtin Ataei was the first student to do this, and Andrew Reinhardt was the second. A special thanks goes to Abtin Ataei for doing a final check on the Problems and Solutions. For the last chapter on LiDAR applications, I felt I did not know the 3D mapping area as well as I should. Dr. Mohan Vaidynathan, my former post-doctorate, works for Harris Corporation (now merged with L3 Technologies) on one of the commercial 3D mappers and volunteered to make an input. Admittedly, he is an advocate of the Geiger-mode version of 3D mapping, as he should be, given where he works, but I knew that. He and his colleagues provided significant input. To balance things out, I did request information from Teledyne Optech and RIEGL as well.

MIT/Lincoln Lab has a nice library of 3D LiDAR images. I would like to thank them for providing one of those images for the book cover.

Finally, I thank Dara Burrows, Senior Editor at SPIE Press, whose tireless work editing this book has made it happen.

This has been an educational experience, and I am pleased with the way the book has turned out. I hope you enjoy it, and I hope many people can use it to learn more about LiDAR technology and systems. I enjoyed writing it, and as I mentioned, learned a lot in certain areas. Perhaps, once in a while it happens that an author learns almost as much by writing a book as a reader learns by reading that book!

Paul McManamon

May 2019

1. P. F. McManamon, P. S. Banks, J. D. Beck, D. G. Fried, A. S. Huntington, and E. A. Watson, "Comparison of flash lidar detector options," *Opt. Eng.* **56**(3), 031223 (2017) [doi: 10.1117/1.OE.56.3.031223].
2. P. F. McManamon, G. Kamerman, and M. Huffaker, "A history of laser radar in the United States," *Proc. SPIE* **7684**, 76840T (2010) [doi: 10.1117/12.862562].
3. V. Molebny, P. F. McManamon, O. Steinvall, T. Kobayashi, and W. Chen, "Laser radar: historical prospective—from the East to the West," *Opt. Eng.* **56**(3), 031220 (2016) [doi: 10.1117/1.OE.56.3.031220].
4. National Academy of Sciences, *Laser Radar: Progress and Opportunities in Active Electro-Optical Sensing*, P. F. McManamon, Chair (Committee on Review of Advancements in Active Electro-Optical Systems to Avoid Technological Surprise Adverse to U.S. National Security), Study under Contract HHM402-10-D-0036-DO#10, National Academies Press, Washington, D.C. (2014).

Chapter 1

Introduction to LiDAR

1.1 Context of LiDAR

LiDAR uses electromagnetic (EM) waves in the optical and infrared wavelengths. It is an active sensor, meaning that it sends out an EM wave and receives the reflected signal back. It is similar to microwave radar, except at a much shorter wavelength. This means that it will have much better angular resolution than radar but will not see through fog or clouds. It is similar to passive electro-optical (EO) sensors in wavelengths, except that it provides its own radiation rather than using existing radiation, and has many more sensing modes due to control over the scene illumination. LiDAR brings its own flashlight and can therefore see at night using near-infrared wavelengths, whereas passive EO sensors have limited capability in the near infrared at night because of insufficient available near-infrared radiation. This means that LiDAR can have increased angular resolution associated with the shorter wavelengths and still operate 24 hours per day.

Figure 1.1 is a diagram showing the EM spectrum that puts LiDAR (and EO devices, in general) into the broader EM-wave context. We see that the visible and infrared spectra have shorter wavelengths than radiowaves and microwaves, but longer wavelengths than x rays and gamma rays. This is a log scale, so the change in wavelength is large. A typical tracking microwave radar might have a frequency of 10 GHz, which corresponds to a wavelength of 3 cm. This is called X-band radar. A typical search radar may have a frequency of 1 GHz and a wavelength of 30 cm. This is called L-band radar. Since a typical eye-safe LiDAR will have a frequency of 200 THz and a wavelength around 1.5 μm , a typical LiDAR will have a wavelength about 20,000 times smaller than the X-band tracking radar, and 200,000 times smaller than the L-band search radar, with corresponding increases in carrier frequency. X rays and gamma rays will be orders of magnitude shorter in wavelength and higher in frequency than visible or infrared EM radiation.

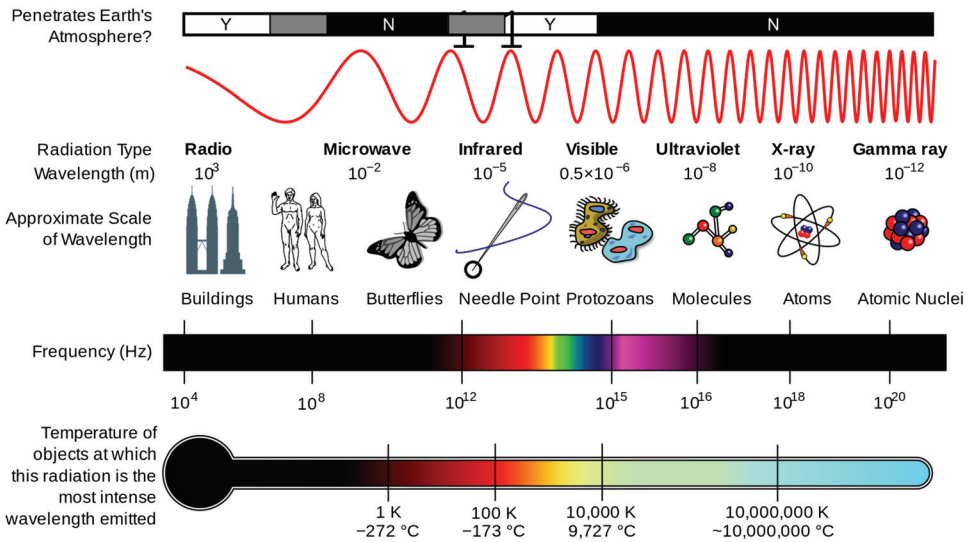


Figure 1.1 The electromagnetic spectrum and the size of common objects compared to the size of a wavelength (adapted from Wikipedia¹ for a NAS study.²)

In general, microwave radar engineers talk in frequency, and optical engineers talk in wavelength. The relationship between wavelength and frequency is

$$c = \lambda\nu, \quad (1.1)$$

where c is the speed of light, λ is the wavelength, and ν is the frequency.

Fog particles are from 1 to 100 μm in diameter, with most particles in the 10- to 15- μm region. Rain drops range from 0.5 to 5 mm in diameter. Truck spray on the highway is likely to have diameter sizes between those of fog particles and rain drops, which will be relevant for autonomous vehicle navigation LiDAR. If the wavelength of an EM wave is significantly longer than the particle size, the wave just flows around particles with little or no attenuation. A 30-cm (or even a 3-cm) microwave signal is significantly larger than rain droplets so will not be significantly attenuated by fog or rain. A 1.5- μm wavelength LiDAR signal will, however, be highly scattered by clouds, fog, or rain. Millimeter-wave radar has a frequency of 95 GHz and a wavelength of 3.16 mm. You can see that millimeter waves at 95 GHz have a wavelength larger than fog but smaller than many rain droplets, so they see through fog well, but not as well through some rain. Fog is worse for LiDAR than rain because fog is made of more particles. A cloud and fog are essentially the same except that fog is sitting on the ground. LiDAR does not penetrate very far through either one. It can penetrate thin clouds with so-called ballistic photons, which are not scattered in the cloud; however, this is exponential decay over a very short range, so LiDAR will not penetrate any

but the thinnest clouds. Even a 10- μm LiDAR would encounter many particles that are as large as or larger than the wavelength so would be significantly attenuated in fog and clouds.

Another comparison for LiDAR is against passive EO sensors. To consider passive EO sensors, we need to think about which EM wavelengths have available radiation that a passive sensor can use. Blackbody radiation is a key aspect of this. Blackbody radiation provides the main signal for passive EO sensors and is the main background noise source for LiDARs. We should therefore be aware of blackbody radiation, which will be covered in the chapter on receivers.

LiDAR is often used as an imaging sensor. It can be for two-dimensional (2D) imaging, similar to the eye or a traditional passive EO sensor, or 3D imaging, where range is measured in each pixel. 3D pixels are usually referred to as voxels. Traditional grayscale, showing intensity variation of the reflected light and therefore a variation in object reflectivity, can also be measured. The color of an object can be measured if more than one wavelength of light is used in the LiDAR. Velocity can be measured either directly using the Doppler shift in frequency due to motion, or by multiple measurements of position. Micro-motion can be measured using the Doppler shift, which is usually measured with a coherent LiDAR. A coherent LiDAR beats the return signal against a local oscillator (LO), which is a sample of the outgoing laser signal. This allows us to measure the phase of the return signal. Optical frequencies are much higher than what any detector can measure, but detectors can measure the beat frequency between two optical waves—the return signal and the LO. This will be further discussed later in this chapter. Coherent LiDAR has an issue with speckle because speckle is a form of interference. When you see laser light reflected from a wall, you will usually see light and dark areas in the reflected spot. This is caused by constructive and destructive interference of narrowband light. A speckled image can be hard to interpret, but if you add many different speckle images with a diversity of speckle, the light and dark areas average out and the image is easier to interpret. Light from the sun or a light bulb has many optical frequencies, so we do not see speckle. The speckle is averaged out. While speckle is usually considered to be an obstacle to laser-based imaging, and usually is averaged out using multiple samples, speckle can also be a feature used in coherent LiDAR to provide additional information about an object.

LiDAR has broad application throughout the military and civilian sectors. Every object has a finite number of observable features that can be exploited by a remote EO sensing system. These features are broadly categorized into the following five types: geometry, surface character, plant noise, effluents, and gross motion. Geometric sensing characterizes the shape of the object in one, two, or three dimensions, including the fully geometrically resolved intensity distributions of the object. Surface character

includes roughness, the spectral and directional distribution of scattered energy, and polarization properties. Plant noises include a variety of vibrations and cyclical motions attributed to the operation of the target. These could be, e.g., signatures associated with piston or turbine engines, transmissions, or other moving components. Effluents include exhaust air, gases, and waste heat. The gross motions are movements of the system, including system translation, rotation, or articulation. All of these types of object discriminants can be sensed by various forms of LiDAR.

LiDAR is a great sensor for identifying objects. One of the reasons for this is that LiDAR can operate at wavelengths similar to what the eye is used to seeing. Due to the reflectance characteristics of microwave radar, it is difficult for the average human to recognize objects using radar images. Scattering in these wavelengths is more specular, resulting in images that are mostly a series of bright spots. People can readily identify objects using visible optical radiation. That is what our eyes use, so we are very familiar with how objects look in the visible wavelength region. One difficulty of passive sensors is they are limited by available radiation. This means that we cannot image objects at extremely long range, as is possible with active sensors such as radar and LiDAR, if we use powerful illumination beams. Also, an active sensor can see at night by illuminating the scene at shorter wavelengths than the available night time radiation, providing a better diffraction-limited resolution at night for a given aperture size.

Another main benefit of LiDAR compared to passive EO sensors is its extremely rich phenomenology due to control of the illumination. Passive sensors provide a 2D image with grayscale or color (or both) in each pixel element. Passive sensors can provide many colors, which can aid in detection or in material identification. If passive sensors frame at a high rate, temporal fluctuations can be observed. A LiDAR can do everything a passive imager can do, although sometimes at a greater cost in photons, sensor size, sensor power, or sensor weight. A LiDAR can provide a 2D angle/angle image but can also provide a 3D image with angle/angle/range information. A LiDAR can directly measure range in each pixel because it controls when light is emitted so can measure range based on time of flight to and from the object in a given pixel. A 3D image can also have grayscale and color if we have enough signal. Coherent LiDAR can measure velocity very accurately. There is a LiDAR mode called laser vibrometry, which can see vibration modes of an object. Reflective surface properties can change the LiDAR return because of speckle. Synthetic-aperture radar (SAR) provides a 2D image in range and cross-range. A synthetic-aperture LiDAR synthetically constructs a larger receive aperture by measuring the field (intensity and phase) of the return in the receive aperture at a given instant. It then moves both the transmit and receive apertures and takes a series of measurements. Because the field is captured in each location, a larger pupil plane image can be assembled and Fourier transformed to obtain a

higher-resolution image. Large effective-pupil-plane images can also be synthesized using multiple receive and/or transmit apertures, a process sometimes referred to as multiple-input, multiple-output (MIMO). LiDAR's rich phenomenology make it an extremely capable sensor.

1.2 Conceptual Discussion of LiDAR

Next, we discuss a conceptual diagram of a LiDAR, shown in Fig. 1.2. A waveform generator creates the laser waveform needed to obtain range or velocity information. A laser would usually provide the illumination, although it is possible to have a LiDAR without a laser. Prior to the invention of the laser, a few LiDAR systems were built. In theory, we could use any light source, but since its invention, the laser has been the light source of choice for LiDAR. This can be a single laser, a seeded laser, or a master oscillator with one or more following laser amplifiers. It could also be an array of lasers. We will talk about those possibilities in Chapter 5. There needs to be a transmit optical aperture that emits the light. This can be the same aperture as the receive aperture, or a different aperture. If it is the same aperture, we call it a monostatic LiDAR, where mono means one aperture. If the transmit and receive apertures are different, we call it a bistatic LiDAR, meaning two apertures. We have to aim the laser at the target we want to view, so we need a pointing method and a way to figure out where to point.

Light has to traverse a medium, usually atmosphere, to arrive at a target. LiDAR can be transmitted through the vacuum of space. LiDAR can also be used through water instead of air or space. Water has significant absorption and sometimes significant scattering, so LiDAR only works well over short ranges in water, possibly on the order of a meter or tens of meters. We do not image though kilometers of water. People usually use blue/green wavelengths to image through water because that is the best spectral window for transmission through

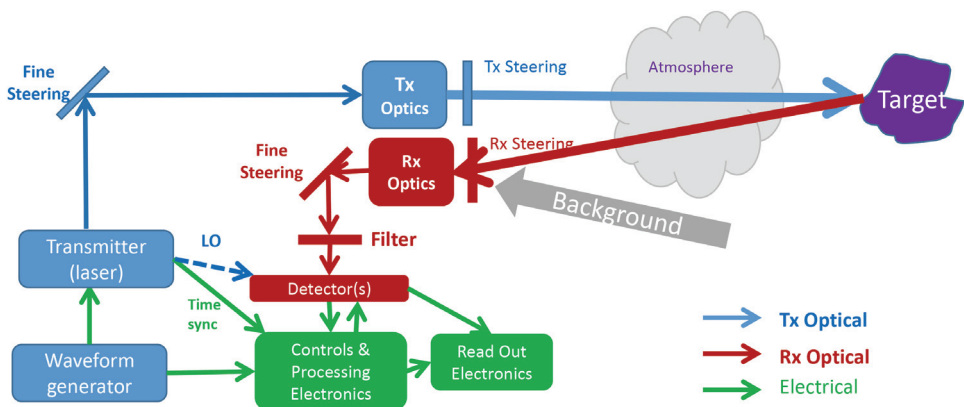


Figure 1.2 LiDAR Conceptual diagram (adapted from Ref. 3).

water. The medical community has also used very short-range LiDAR through human tissue. Usually medical LiDAR used in humans is in a tomographic imaging mode, where the laser illuminates from one angle, but multiple angles of the scattered light are then captured to develop a picture of the human tissue. There is significant scattering in the human body, and just like in water, some wavelengths transmit better than others. Red, the color of blood, transmits relatively well through the body. If you take a red laser pointer and a green laser pointer into a dark room and put each against the bottom of your index finger in turn, you will see much more red light coming through your finger than green light. LiDAR light bounces off the target and traverses the medium again until it is captured by the receiver optical aperture in the pupil plane, which also needs to point at the target. If we use a lens to focus the light captured by the receive aperture, then we convert to the image plane.

Alternatively, if we can capture or estimate the field at the aperture (the pupil plane), we can Fourier transform the field at the pupil plane to form an image. One of the nice things about capturing the full field (phase and intensity) in the pupil plane is that a larger pupil-plane aperture can be synthesized and then Fourier transformed to make a higher-resolution image. To measure the full field in the pupil plane rather than just the intensity requires that we beat the return signal against another signal that (as mentioned) we call the local oscillator (LO). Using a detector array, we can make an image with a single pulse (flash imaging), but we also can scan a small optical beam and develop an angle/angle image over time while using one or a small number of detectors.

Optical wavelengths are at very high frequencies, so we cannot directly measure phase. No detector is fast enough to detect 200 THz (1.5- μm light) or other similar very high frequencies. To detect temporal phase, we can use an LO that interferes with the return signal on the detector. We refer to the LO beating against the return signal. We can then measure the beat frequency, which allows us to measure the phase of the return light as well as the intensity (we call this coherent LiDAR). If the LO is perfectly stable, the phase change in the beat frequency is the same as the phase of the carrier frequency, which is the returned signal, so in coherent LiDAR, we can capture phase. We need a timing signal from the transmitter to determine range by measuring time of flight of the laser pulse to and from the target. We know the speed of light in vacuum and in air, so we can calculate the distance to an object. The signal generated by the detector is digitized and then processed to make an image or to generate information such as velocity or vibration frequency based on the return Doppler shift.

1.3 Terms for Active EO Sensing

In this book we use the term LiDAR because it is most popular, but other terms that have been used for active EO sensing are shown in Fig. 1.3. Historically,

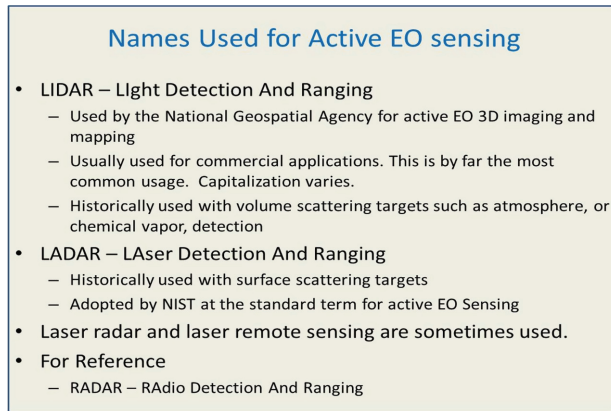


Figure 1.3 Terms for active EO sensing (reprinted from Ref. 2).

the term LiDAR has been used by the active EO sensing community in conjunction with measuring volume-based targets such as aerosols, and ladar has been used in conjunction with surface-based reflections. Sometimes people would refer to soft targets for volume scattering and hard targets for surface scattering. LiDAR has been the term used more often in commercial applications and therefore has more widespread usage. There have also been variations in the letters that are capitalized in the acronym. The most popular version is lidar, then LIDAR, followed by LiDAR, and LADAR, but LiDAR has recently grown in popularity due to its use in the commercial sector, such as auto LiDAR. Often the various terms are used almost interchangeably, depending on who is using them. This can cause confusion.

Figure 1.4 is a Google Ngram that charts the usage of LiDAR versus ladar.⁴

You can see that the term LiDAR, grouping all the various capitalizations, was much more widely used than the term ladar during the period

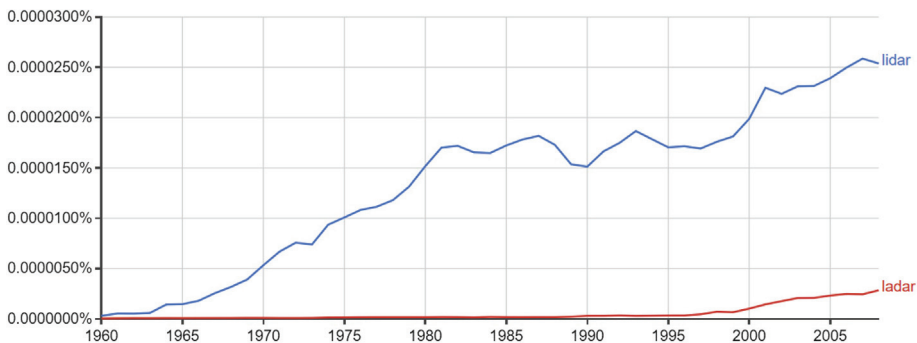


Figure 1.4 Google Ngram comparing use of the term LiDAR to use of the term ladar, ignoring capitalization. The graph stops at 2008.⁴

covered by the Ngram. As a result, people are more likely to understand what we mean with respect to active EO sensing if we use the term LiDAR. Finally, this book uses LiDAR as both a technology and a specific instrument or system.

1.4 Types of LiDARs

Many types of LiDARs will be discussed in Chapter 4, but this section provides a short preview. Range in a LiDAR is measured by timing how long it takes light to hit an object and return. Range resolution is given by

$$\Delta R = \frac{c}{2B}, \quad (1.2)$$

where ΔR is the range resolution, c is the speed of light in the intervening medium, and B is the system bandwidth, which could be limited by the transmit signal bandwidth or the receiver bandwidth (which can be limited by the detector or its electronics). Angle information is detected by one or a number of detectors moving in angle, or by an array of detectors sampling the field of view (FOV). Angular resolutions can either be limited by the detector angular subtense (DAS) or by diffraction. Figure 1.5 shows various sampling possibilities; the middle curve represents the case where the DAS is about the same as the point spread function (PSF) of the optical aperture. We could also oversample the PSF as shown on the right, or under sample it as shown on the left.

A LiDAR that only measures one dimension (range) is called a range-only LiDAR or a 1D LiDAR. Another LiDAR is like a passive imager in that it measures both azimuth and elevation, but does not measure range in each pixel. A 2D LiDAR can be range gated to a certain range region of interest. This can reduce noise and distractions from ranges that are not in the region of interest. For example, in fog, backscatter from closer ranges could obscure the return from the range of interest. A 2D LiDAR provides its own

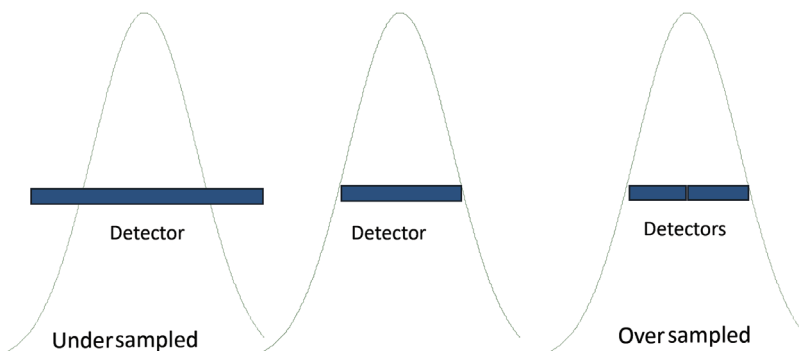


Figure 1.5 Various sampling possibilities (reprinted from Ref. 3).

illumination, as do all LiDARs, which is an advantage compared to passive imagers. A common type of LiDAR today is a 3D LiDAR, which measures angle/angle/range. A 3D image can be just three dimensions with no grayscale, or it can measure grayscale as well, meaning that the relative intensity of the returns vary across the image. Some areas of the image reflect more strongly than other areas. The number of grayscale levels is given by

$$N_{\text{gs}} = 2^N, \quad (1.3)$$

where N is the number of bits of grayscale, and N_{gs} is the number of levels of grayscale. Table 1.1 shows that we will have 64 levels of grayscale with 6 bits of grayscale and 8 levels with 3 bits. In direct detection systems, two types of information are typically recovered. One is the range from the sensor to the target on a pixel-by-pixel basis, which is often called a point cloud. Here, the range information is gathered as a function of position (often through some form of timing circuitry) on the receiver focal plane. Hence, the contrast information that is provided from pixel to pixel is a variation in range information. The other type of information that can be gathered is reflectance information. The contrast from pixel to pixel in this case is the number of returned photons for each pixel (e.g., irradiance). This is a measurement of grayscale.

Polarization and color (wavelength) are other dimensions that can be measured. A coherent LiDAR, which measures the phase of the return signal as well as amplitude, can measure the velocity of an object by measuring the Doppler shift, a change in return frequency that results from an object's velocity. Historically, people would use a train approaching and leaving a station to explain the frequency change due to velocity to or away from an object. This worked because at the time people were familiar with the change in pitch as the train approached and passed the station. Angle measurement can be made using an aperture that is synthesized by sampling the pupil plane field

Table 1.1 Number of grayscale levels N_{gs} versus number of bits of grayscale N .

N	N_{gs}
1	2
2	4
3	8
4	16
5	32
6	64
7	128
8	256
9	512
10	1025

in many locations and then constructing a larger pupil plane field sample, which can be Fourier transformed to obtain the image. Synthetic-aperture LiDAR (SAL) is one form of a synthesized LiDAR aperture. Other forms can include multiple physical apertures on receive only or on both receive and transmit. As mentioned earlier, LiDARs that use multiple receive and transmit apertures are called MIMO, for multiple input, multiple output. To date, the term MIMO has been used much more in microwave radar than in LiDAR.

1.4.1 Some LiDARs for surface-scattering (hard) targets

LiDAR can be used for many different applications because it is such a rich sensing approach. 3D LiDAR is used for 3D mapping. 2D LiDAR images look very much like conventional EO images. As mentioned, we can have range-only, or 1D, LiDAR. We can also have coherent Doppler LiDAR that measures velocity and vibration. A well-known application of LiDAR is the driverless car. All of the DARPA Grand Challenge finishers used at least one LiDAR. Almost all of the other driverless car developers are using LiDAR. Admittedly, the Tesla driverless car in which a passenger was killed did not have LiDAR, but it was not designed for true driverless function. Drivers are supposed to maintain alertness in case they are needed. Police speed detection is another common LiDAR use. LiDAR can pick out one vehicle in a cluttered traffic situation using a system that can be mounted in a small camera.

Small UAVs such as the Amazon UAV use LiDAR. The Microsoft[®] Kinect game system is a relatively new, very widespread use of a simple LiDAR. Forestry LiDAR is unique in its ability to measure the vertical structure of forest canopies, map the ground beneath the forest, and estimate canopy bulk density. LiDAR can map flood plains and can map the ground in coastal areas in and out of the water.

Transportation corridors can be 3D mapped to support high-scale engineering mapping accuracy. The military can use 3D map data for route planning to avoid being seen from a certain location, and for precise object identification. LiDAR's high accuracy means that a quick survey will give precise volumetric measurements for oil and gas exploration and for quarrying.

LiDAR can provide the data for cellular network planning to determine line of sight and viewshed for proposed cellular antenna. LiDAR allows any physical object to be re-created in a computer environment, or with a 3D printer, so the advent of 3D printing should increase demand for LiDAR. LiDARs can make recording the scene of accidents and crimes quick, easy, and precise. LiDAR has been used in archeology mapping. LiDAR is a useful tool when designing and constructing new buildings and in determining the location of specific items within the interior of a room for licensing regulations and to provide proof of compliance. LiDAR can enable surveys to be taken of places

that may be considered too dangerous for humans to enter. A robotic vehicle can be sent down sewers and can take detailed surveys of the interior of the system. This is only a small subset of the surface-scattering LiDAR applications, which are limited only by people's imagination and inventiveness.

1.4.2 Some LiDARs for volume-scattering (soft) targets

Wind speed can be measured either by the Doppler shift along the path from the LiDAR or from multiple accurate range measurements. Doppler LiDAR is used to measure wind speed along the beam by measuring the frequency shift of the backscattered light. This can be for military applications such as air drop of cargo or to map the wind fields around an airport or around a set of wind turbines, or near sailboats in a sailboat race. Differential absorption LiDAR (DIAL) can be used to detect range-resolved trace amounts of gases such as ozone, carbon dioxide, or water vapor. The LiDAR transmits two wavelengths: an online wavelength that is absorbed by the gas of interest and an offline wavelength that is not absorbed. For example, ARPA-E has a recent program called MONITOR (Methane Observation Networks with Innovative Technology to Obtain Reductions) to detect methane gases. The differential absorption between the two wavelengths is a measure of the concentration of the gas. Raman LiDAR is also used for measuring the concentration of atmospheric gases. Raman LiDAR exploits inelastic scattering to single out the gas of interest. A small portion of the energy of the transmitted light is deposited in the gas during the scattering process, which shifts the scattered light to a longer wavelength by an amount that is unique to the species of interest.

Laser-induced fluorescence (LIF) LiDARs are similar to Raman LiDARs in that they only require that the entity to be detected be present in the atmosphere or on the surface of a target of interest. Unlike Raman LiDARs, however, the LIF systems seek to create real transitions in the entity through excitation to higher electronic levels. Laser-induced breakdown spectroscopy (LIBS) is part of the volume-scattering discussion because it involves first vaporizing a small amount of material and then using spectroscopy to identify the vaporized material. The Curiosity spacecraft on Mars uses a LIBS sensor to remotely determine rock type.

1.5 LiDAR Detection Modes

An optical detector does not respond to the 200- to 600-THz carrier frequency of 1.5- to 0.5- μm light. When light hits a detector, it generates a voltage equal to the square of the intensity of the impinging light. In ideal direct detection, only the LiDAR return hits the detector, causing a response equal to the square of the intensity of the impinging light. In coherent LiDAR, the return signal beats against a sample of the emitted signal, which we call the local

oscillator (LO). In this case, the detector can respond to the real portion of the beat frequency, or difference frequency, between the return signal and the LO:

$$I = 2 E_{\text{sig}} E_{\text{LO}} \cos[-j(\omega_{\text{sig}} - \omega_{\text{LO}})], \quad (1.4)$$

where it can be seen that, in temporal heterodyne detection, the LO and return signal are spatially aligned to interfere on the detector. For the temporal heterodyne mode, the LO and the return signal must be spatially matched, or else high-spatial-frequency fringes will lower heterodyne mixing efficiency. This means that both the direction of propagation as well as the phase front of each beam must be matched. The frequency of the LO is offset so that we can tell the direction of target velocity and to reduce $1/f$ noise. If there is no frequency offset, temporal heterodyne LiDAR is called homodyne LiDAR. This beating is shown in Fig. 1.6.

In spatial heterodyne detection, also called digital holography, the LO and the return signal are slightly misaligned, as shown in Fig. 1.7. For simplicity, this figure does not show the slightly offset beams after they are combined and before they hit the detector. The tilt between the LO and the return signal creates fringes that can be sampled by a detector array. If the angular tilt is too large, the fringes will be too rapid and will average out across a detector. In phase shift interferometry, the reflected wave is mixed with a LO of the same frequency. The interferogram is measured on a 2D detector array. Multiple interferograms are recorded in which a known piston phase has been applied to the LO. Three or more interferograms are processed to extract the field amplitude and phase.

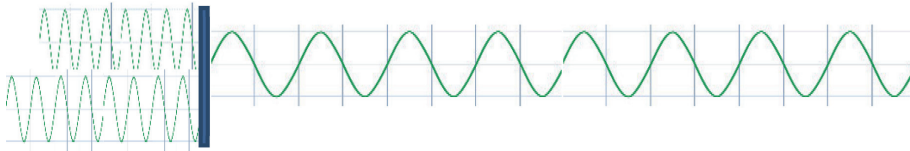


Figure 1.6 Beat frequency for temporal heterodyne detection (reprinted from Ref. 3).

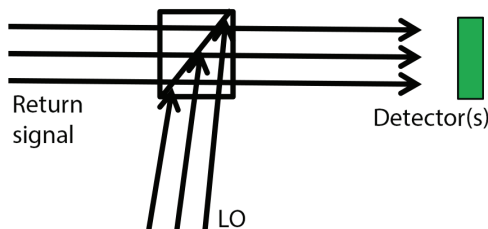


Figure 1.7 Angularly offset LO for spatial heterodyne detection, or digital holography (reprinted from Ref. 3).

1.6 Flash LiDAR versus Scanning LiDAR

Spatial coherence uses the angular width of the laser beam. For LiDARs that have a single detector, the laser beam must illuminate the area covered by the single detector. If the LiDAR uses a detector array, which we refer to as flash LiDAR, then the laser illuminates an area as large in angle as the detector array, so the laser beam is wider in angle. The diffraction limit provides the smallest possible laser beam divergence. The full beam width, half maximum diffraction limit is

$$\theta \approx \frac{1.03 \lambda}{D}, \quad (1.5)$$

where D is the diameter of the transmit aperture. If the transmit aperture is the same aperture, or the same size, as the receive aperture, then for flash imaging we do not need high spatial coherence. Our transmit beam does not need to be single mode because the illuminated area can be much larger than the diffraction limit. Flash imaging is shown in Fig. 1.8.

Many LiDAR illumination beams are Gaussian, but a flat topped beam is often desirable. A super-Gaussian beam has a flatter top than a Gaussian beam, allowing for a more uniform illumination pattern. For a Gaussian beam where $N = 2$, and for a super-Gaussian beam, where $N > 2$,

$$f(x) = ae^{-\frac{(x-b)^N}{2c^2}}, \quad (1.6)$$

where a is the magnitude of the Gaussian beam, b is the offset from zero, and c is the width of the Gaussian beam. Figure 1.9 shows a Gaussian beam and a super-Gaussian shape. With a finite-sized transmit aperture, you can clip less energy from the laser beam with any flatter-topped beam shape, including variously powered super-Gaussian shapes. A Gaussian beam concentrates its energy in the middle of the point spread function (PSF) more than a super-Gaussian, or flat top, PSF, but it also spreads some energy into a wider angle, where it might be clipped by an aperture. A flat-top beam spreads energy across the aperture, but then the energy decreases quickly, so not as much energy is clipped by an aperture.



Figure 1.8 Flash imaging (reprinted from Ref. 3).

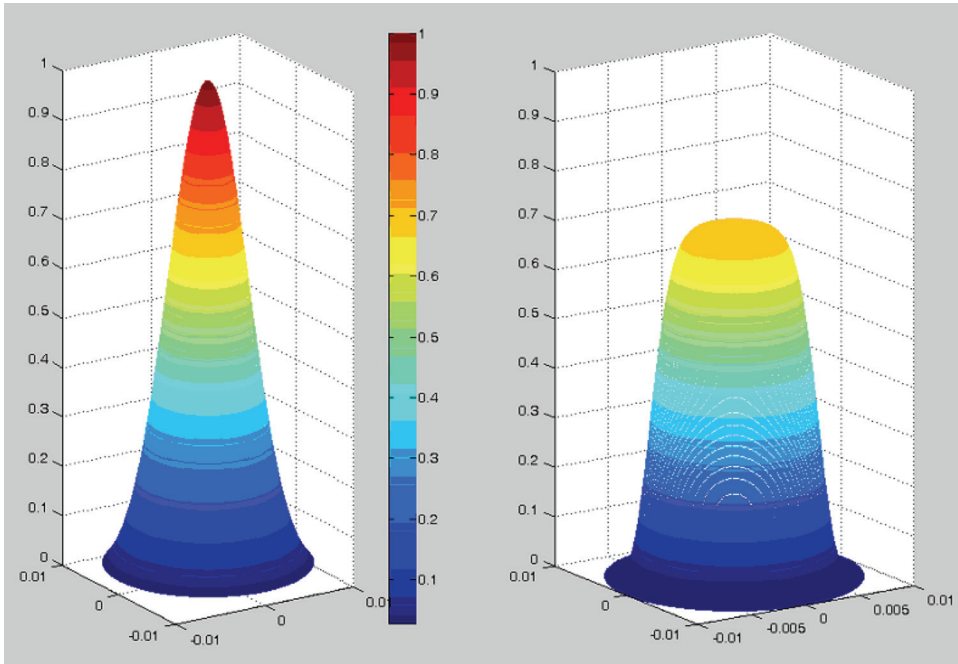


Figure 1.9 Gaussian (left) versus super-Gaussian (right) beam shapes (reprinted from Ref. 3).

1.7 Eye Safety Considerations

Laser radiation can damage the eye by burning the retina after magnification, or by burning the surface of the eye (see Fig. 1.10). The eye has significant magnification when it focuses light on the retina, so the damage threshold for light entering the eye and focusing on the retina is much lower than the damage threshold for burning the surface of the eye. Lasers beyond $\sim 1.5 \mu\text{m}$,

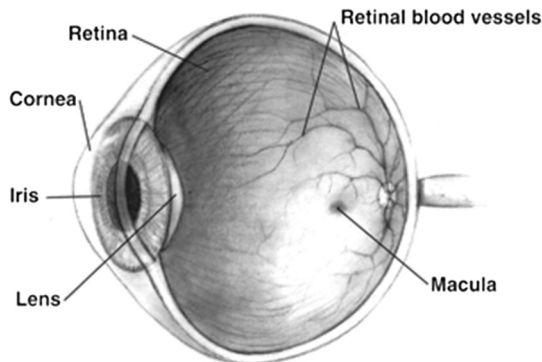


Figure 1.10 A schematic image of the eye (from Wikipedia: Laser safety. Created by Han-Kwang Nienhuys and released under license CC-BY-2.5).

or below about $0.4 \mu\text{m}$, are safer because water in the eye absorbs wavelengths in these regions, preventing light from focusing on the retina. You can still burn the surface of the eye, but without the large increase in irradiance resulting from focusing the light. It is rare for LiDARs to operate below $0.4 \mu\text{m}$ for better eye safety, but it is common for them to operate at $1.5 \mu\text{m}$ or longer. A slight decrease in the maximum allowed flux levels is seen as you move to operation wavelengths longer than $1.5 \mu\text{m}$. This is because the eye absorbs the light that is closer to the surface at longer wavelengths, so the light is absorbed in a smaller volume of eye tissue. A smaller volume will heat up sooner. At $1.5 \mu\text{m}$, the light is all absorbed before it hits the retina, but it is absorbed in a volume of most of the eye. At $10 \mu\text{m}$, water is more absorptive, so it is absorbed near the surface of the eye.

Figure 1.11 shows the maximum permissible exposure (MPE) for various wavelengths. MPE is given in units of energy per area (J/cm^2). Often this level of exposure in ten seconds is used as a threshold. A scanning laser hits the eye only for a brief time period, whereas the laser in a flash-illuminated LiDAR illuminates the eye for a much longer time period. Because a scanning laser does not illuminate the eye for as high a percentage of time, the laser can be more powerful without exceeding the eye safety threshold. From Fig. 1.11, we can see the effect of operating in a higher-eye-safety wavelength region. The maximum permissible laser flux is around $1.5 \mu\text{m}$. Depending on the laser pulse width, the reduction in allowed laser flux can be anywhere from 3 to 8 orders of magnitude at $1.5 \mu\text{m}$ compared to that of the visible light that will hit the retina. The time numbers in Fig. 1.11 are pulse widths. As mentioned, people generally assume a 10-s exposure of the eye and calculate the total energy absorbed by the eye, and then compare this to Fig. 1.11 for a given pulse width. If the laser scans, it can

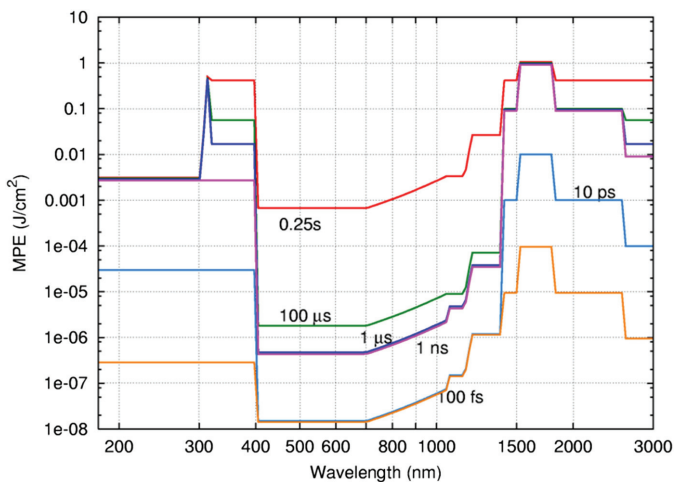


Figure 1.11 Laser safety thresholds (MPE) versus wavelength (from Wikipedia: Laser safety. Created by Dahn and released under license CC-BY-2.5).

reduce the total energy absorbed by the eye because the laser will only be illuminating the eye during a portion of the time.

1.8 Laser Safety Categories

Since the early 1970s, lasers have been grouped into four classes and a few subclasses according to wavelength and maximum output power. The classifications categorize lasers according to their ability to produce damage to people. There are two classification systems: the “old” system, which was used before 2002, and the “revised” system, which started being phased in after 2002. The latter reflects the greater knowledge of lasers that has been accumulated since the original classification system was devised and permits certain types of lasers to be recognized as having a lower hazard than was implied by their placement in the original classification system. Figure 1.12 shows the laser safety classes:

- Class 1 lasers are safe unless focused.
- Class 2 lasers only cover the spectral range of 400–700 nm. They are safe because of the blink reflex, which only occurs at those spectral regions because you won’t blink if you don’t see it. Class 2 lasers are 1 mW continuous wave (cw) or less.
- Class 3R lasers are less than or equal to 5 mW cw. They are safe if handled properly.
- Class 3B laser operators may need goggles. These lasers can be up to 30 mW.
- Class 4 lasers can burn the skin as well as damage the eye.

Note that some laser pointers are more than 5 mW. Many of those you can order on the Internet are higher than 5 mW. Be careful!! For LiDAR, the

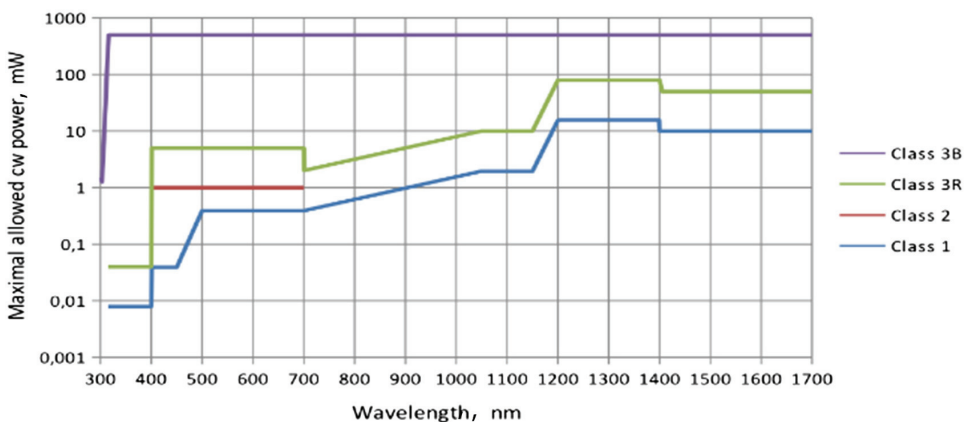


Figure 1.12 Laser safety classes (from Wikipedia: Laser safety. Created by Dahn and released under license CC-BY-2.5).

MPE values discussed previously are more important than the laser classifications because they are given per area of aperture.

1.9 Monostatic versus Bistatic LiDAR

A way to isolate the transmit and receive functions is to use a different telescope for each function such that the backscatter in the optical system is eliminated. The only backscatter you then have to worry about comes from scattering off of the aerosols close to the LiDAR. If the transmit and receive apertures are two separate apertures, we call that a bistatic LiDAR, as shown in Fig. 1.13. The transmit, or illumination, aperture does not have to be the same size as the receive aperture, nor in the same place. A laser designator is a bistatic LiDAR illuminator with the seeker as the receiver, even though people do not think of laser designator systems as being a bistatic LiDAR.

One reason for using monostatic LiDARs is to save weight and space by not having a second aperture for illumination; however, with bistatic illumination often you can have an illumination aperture that is much smaller than the receive aperture, reducing the size, weight, and power impact of having two apertures. This is the case for flash LiDAR, where the area illuminated is larger than the area viewed by a single DAS. Having a small transmit aperture for illumination is especially important for coherent LiDAR so that the phase across the illuminated region is constant. Also, as will be discussed in Chapter 4, multiple-input, multiple-output (MIMO) LiDARs provide the benefits of having more than one transmitter and more than one receiver. Any MIMO LiDAR is inherently bistatic. Often in a MIMO LiDAR, the transmit apertures will be smaller than the receive apertures.

A monostatic LiDAR uses the same aperture for transmit and receive. As a result, we need to provide isolation between the transmitter and receiver, or backscatter from the transmitted pulse will blind the receiver. Various methods of providing isolation are discussed next.

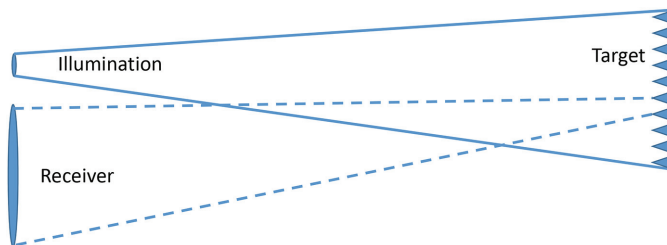


Figure 1.13 Bistatic LiDAR illumination diagram (reprinted from Ref. 2).

1.10 Transmit/Receive Isolation

High-power backscattered laser radiation can blind or damage the receiver, so we need to isolate the high-power transmitted laser waveform from the receiver. One way to isolate the receiver from the transmitter is to have a bistatic LiDAR with separate apertures. If the LiDAR has a pulsed-cycle, or low-duty cycle, transmitter, then another way to isolate the receiver from the transmitter is to keep the receiver off while the laser is transmitted. With the receiver off, we do not have to worry about the amount of isolation between the transmitter and the receiver. We will see, however, that there are reasons we might want a high-duty-cycle or continuous-wave (cw) waveform. In this case, we need a way to prevent emitted laser power from being backscattered into the receiver. The most common way to do this is to use polarization (see Fig. 1.14). If we transmit a linearly polarized laser beam, we can isolate it using a polarizing beamsplitter. A quarter-wave plate will convert linear polarization to circular polarization. When that circular polarization bounces off of an object, most of the light will reverse its handedness. On return, the opposite-handedness circular-polarization beam will be converted to the opposite linear polarization of the laser and will be transmitted through the polarizing beamsplitter to the receiver. This polarization method of transmit/receive isolation can achieve up to 40–45 dB of isolation with careful design. Isolation of up to 40–45 dB is a rejection factor of between 10,000 and 30,000. The backscatter that hits the camera will come from the quarter-wave plate and the transmit telescope. Quality engineering will reduce this scatter.

1.11 Major Devices in a LiDAR

There are three main components in a LiDAR: the laser source, the receiver, and the optical systems for pointing the LiDAR. Each of these components are briefly discussed next and will be discussed in detail in Chapters 5, 6, and 7.

1.11.1 Laser sources

As stated earlier, while it is possible for a LiDAR to be built with a light source other than a laser, this is highly unlikely. At the current time, virtually

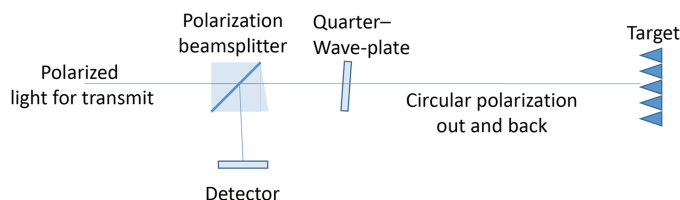


Figure 1.14 Transmit/receive isolation approach using polarization (reprinted from Ref. 3).

all LiDARs use either a diode laser or a diode-pumped solid state laser. Diode-pumped solid state lasers can be divided into bulk solid state lasers and fiber lasers. Diode lasers can be very efficient and can be inexpensive. However, they do not store energy so cannot be Q switched, they tend to have a broad laser line width, and they tend to have a broad beam. Because of these characteristics, it is often useful to use diode lasers to pump a solid state medium that can be Q switched to obtain higher peak power. The solid state laser may also have narrower linewidth and beam divergence closer to the diffraction limit. Fiber lasers tend to be limited in peak power because of limited gain area in the fiber. This means that fiber lasers are normally used with higher-duty-cycle LiDARs.

1.11.2 Receivers

LiDAR receivers can be a single detector or an array of detectors. In the early days of LiDAR, we often used single detectors, but more recently, high-bandwidth arrays have become available that can measure range in each pixel based on the time of return of a reflected laser pulse. Also, some LiDAR implementations do not require high-bandwidth detectors. To increase the signal-to-noise ratio (SNR) in the receiver, two main approaches have been used. For coherent LiDAR, increasing the intensity of the LO increases the SNR in the receiver. For any LiDAR, but primarily for those used for direct detection, we can make use of gain on the receiver to increase the receiver SNR. While the gain can come prior to detection, it is usually done in a detector or a detector array after detection by generating multiple electrons per received photon. Linear-mode avalanche photodiodes (LAPDs) have a linear relationship between the number of received photons and the number of generated electrons, while Geiger-mode APDs always generate a maximum number of electrons when one or more photons is received.

1.11.3 Apertures

We need optics in a LiDAR, and we need a method of pointing both the transmitter and the receiver. As discussed above, a single aperture can be used for both the transmitter and the receiver, or these apertures can be separate. When we point an optical system for transmit or for receive, we use either mechanical or nonmechanical pointing approaches. A simple pointing scheme can be a mirror that can be tilted. There are many mechanical approaches to pointing an optical system. The effect of these mechanical pointing systems is to change the tilt of the optical wavefront. If we can change the tilt of the optical wavefront without moving a mechanical device, we call this nonmechanical beam pointing. Over the past few decades, many nonmechanical beam-pointing approaches have been explored.^{5,6} Some of these

approaches use optical phased arrays, which are similar to the phased arrays in microwave systems that can change the tilt of the phase front of an electromagnetic wave. In Chapter 7 both mechanical and nonmechanical beam-pointing approaches will be discussed in detail.

1.12 Organization of the Book

This book has 12 chapters. The introduction you have just read is the first chapter. Chapter 2 looks back at LiDAR history. This chapter summarizes some of the information in Ref. 7 and includes some information from Ref. 8 that is not included in Ref. 4. The author of this book coauthored Ref. 6 and was a very active coauthor in Ref. 5.

Chapter 3 develops the LiDAR range equation and link budget. It shows how to calculate the number of returned photons when the LiDAR aperture, laser power, atmospheric conditions, and other parameters are known.

Chapter 4 discusses the types of LiDAR. Chapter 5 discusses lasers for LiDAR application and LiDAR waveforms. Chapter 6 discusses LiDAR receiver technology; to calculate the range of a given LiDAR, you will need information from both Chapters 3 and 6. Chapter 7 discusses apertures, pointing technology, and LiDAR optics.

Chapter 8 addresses LiDAR processing, and Chapter 9 presents LiDAR testing. Chapter 10 discusses metrics for evaluating LiDAR, and Chapter 11 discusses some LiDAR applications.

Problems and Solutions

1-1. Calculate how many 1550-nm photons will be contained in 1 nJ of energy.

1-1 Solution:

$$c = 3 \times 10^8 \text{ m/s,}$$

$$h = 6.63 \times 10^{-34} \text{ J s,}$$

$$\lambda = 1550 \text{ nm,}$$

$$E = 1 \text{ nJ.}$$

First, consider how much energy is in a single photon:

$$E_p = \frac{hc}{\lambda}.$$

Second, consider how much energy we are given in this problem: $E = 1 \text{ nJ}$. Therefore,

$$N = \frac{E}{E_p} = \frac{E\lambda}{hc} = \frac{(1 \times 10^{-9} \text{ J})(1.55 \times 10^{-6} \text{ m})}{(6.626 \times 10^{-34} \text{ J s})(3 \times 10^8 \text{ m/s})},$$

$$N = 7.798 \times 10^9 \text{ photons.}$$

1-2. Assuming that the sun is a blackbody, calculate the ratio of flux from the sun at a wavelength of 900 nm to flux from the sun at 1550 nm.

1-2 Solution:

$$T = 6050 \text{ K,}$$

$$\lambda_1 = 900 \text{ nm,}$$

$$\lambda_2 = 1550 \text{ nm,}$$

$$k = 1.38 \times 10^{-23} \text{ J/K,}$$

$$c = 3 \times 10^8 \text{ m/s,}$$

$$h = 6.63 \times 10^{-34} \text{ J s.}$$

Blackbody flux is given as

$$L_1 = \frac{2hc^2}{\lambda_1^5} \left[\exp\left(\frac{hc}{\lambda_1 kT}\right) - 1 \right]^{-1},$$

$$L_2 = \frac{2hc^2}{\lambda_2^5} \left[\exp\left(\frac{hc}{\lambda_2 kT}\right) - 1 \right]^{-1}.$$

Next, consider the ratio of the two fluxes:

$$\frac{L_2}{L_1} = \frac{\left(\frac{2hc^2}{\lambda_2^5} \left[\exp\left(\frac{hc}{\lambda_2 kT}\right) - 1 \right]^{-1}\right)}{\left(\frac{2hc^2}{\lambda_1^5} \left[\exp\left(\frac{hc}{\lambda_1 kT}\right) - 1 \right]^{-1}\right)} = \frac{\lambda_1^5 \left[\exp\left(\frac{hc}{\lambda_1 kT}\right) - 1 \right]}{\lambda_2^5 \left[\exp\left(\frac{hc}{\lambda_2 kT}\right) - 1 \right]},$$

$$\frac{L_2}{L_1} = \frac{(9 \times 10^{-7} \text{ m})^5 \left[\exp\left(\frac{(6.63 \times 10^{-34} \text{ J s})(3 \times 10^8 \text{ m/s})}{(9 \times 10^{-7} \text{ m})(1.38 \times 10^{-23} \text{ J/K})(6050 \text{ K})}\right) - 1 \right]}{(1.55 \times 10^{-6} \text{ m})^5 \left[\exp\left(\frac{(6.63 \times 10^{-34} \text{ J s})(3 \times 10^8 \text{ m/s})}{(1.55 \times 10^{-6} \text{ m})(1.38 \times 10^{-23} \text{ J/K})(6050 \text{ K})}\right) - 1 \right]}$$

$$= 0.2371.$$

So, the ratio of blackbody flux from the sun at 1550 nm to that at 900 nm is 23.71%.

1-3. For a 300-deg blackbody, calculate the ratio of flux at a wavelength of 10 μm to the flux available at a wavelength of 4.8 μm . Then compare the flux at 4.8 μm to the flux at 3.8 μm .

1-3 Solution:

$$\begin{aligned}
T &= 300 \text{ K}, \\
\lambda_1 &= 10 \text{ } \mu\text{m}, \\
\lambda_2 &= 4.8 \text{ } \mu\text{m}, \\
\lambda_3 &= 3.8 \text{ } \mu\text{m}, \\
k &= 1.38 \times 10^{-23} \text{ J/K}, \\
c &= 3 \times 10^8 \text{ m/s}, \\
h &= 6.63 \times 10^{-34} \text{ J s}.
\end{aligned}$$

Blackbody flux is given as

$$\begin{aligned}
L_1 &= \frac{2hc^2}{\lambda_1^5} \left[\exp\left(\frac{hc}{\lambda_1 kT}\right) - 1 \right]^{-1}, \\
L_2 &= \frac{2hc^2}{\lambda_2^5} \left[\exp\left(\frac{hc}{\lambda_2 kT}\right) - 1 \right]^{-1}, \\
L_3 &= \frac{2hc^2}{\lambda_3^5} \left[\exp\left(\frac{hc}{\lambda_3 kT}\right) - 1 \right]^{-1}.
\end{aligned}$$

Next, consider the ratio of the two fluxes:

$$\begin{aligned}
\frac{L_2}{L_1} &= \frac{\left(\frac{2hc^2}{\lambda_2^5} \left[\exp\left(\frac{hc}{\lambda_2 kT}\right) - 1 \right]^{-1}\right)}{\left(\frac{2hc^2}{\lambda_1^5} \left[\exp\left(\frac{hc}{\lambda_1 kT}\right) - 1 \right]^{-1}\right)} = \frac{\lambda_1^5 \left[\exp\left(\frac{hc}{\lambda_1 kT}\right) - 1 \right]}{\lambda_2^5 \left[\exp\left(\frac{hc}{\lambda_2 kT}\right) - 1 \right]}, \\
\frac{L_2}{L_1} &= \frac{(1 \times 10^{-5} \text{ m})^5 \left[\exp\left(\frac{(6.63 \times 10^{-34} \text{ J s})(3 \times 10^8 \text{ m/s})}{(1 \times 10^{-5} \text{ m})(1.38 \times 10^{-23} \text{ J/K})(300 \text{ K})}\right) - 1 \right]}{(4.8 \times 10^{-6} \text{ m})^5 \left[\exp\left(\frac{(6.63 \times 10^{-34} \text{ J s})(3 \times 10^8 \text{ m/s})}{(4.8 \times 10^{-6} \text{ m})(1.38 \times 10^{-23} \text{ J/K})(300 \text{ K})}\right) - 1 \right]} \\
&= 0.2371.
\end{aligned}$$

So, the ratio of blackbody flux from an object of 300 K temperature at 10 μm to that at 4.8 μm is 21.37%.

Similarly,

$$\begin{aligned}
\frac{L_3}{L_2} &= \frac{\lambda_2^5 \left[\exp\left(\frac{hc}{\lambda_2 kT}\right) - 1 \right]}{\lambda_3^5 \left[\exp\left(\frac{hc}{\lambda_3 kT}\right) - 1 \right]}, \\
\frac{L_3}{L_2} &= \frac{(4.8 \times 10^{-6} \text{ m})^5 \left[\exp\left(\frac{(6.63 \times 10^{-34} \text{ J s})(3 \times 10^8 \text{ m/s})}{(4.8 \times 10^{-6} \text{ m})(1.38 \times 10^{-23} \text{ J/K})(300 \text{ K})}\right) - 1 \right]}{(3.8 \times 10^{-6} \text{ m})^5 \left[\exp\left(\frac{(6.63 \times 10^{-34} \text{ J s})(3 \times 10^8 \text{ m/s})}{(3.8 \times 10^{-6} \text{ m})(1.38 \times 10^{-23} \text{ J/K})(300 \text{ K})}\right) - 1 \right]} \\
&= 0.2309.
\end{aligned}$$

So, the ratio of blackbody flux from an object of 300 K temperature at 4.8 μm to that at 3.8 μm is 23.09%.

1-4. For a 10-nm-wide spectral band at a wavelength of 1.5 μm , what is the flux per nanometer in one square meter $B_{\text{sqm-nm}}$ on Earth?

1-4 Solution: The flux per unit area on Earth is given by

$$B_{\text{sqm-nm}} = \frac{LR_s^2}{R_e^2},$$

where R_s is the radius of the sun, R_e is the radius of the earth, and L is the blackbody radiation of the sun, which is given as

$$L = \frac{2hc^2}{\lambda^5} \left[\exp\left(\frac{hc}{\lambda kT}\right) - 1 \right]^{-1},$$

$$L = \frac{2(6.63 \times 10^{-34} \text{ J s})(3 \times 10^8 \text{ m/s})^2}{(1.5 \times 10^{-6} \text{ m})^5}$$

$$\left\{ \exp\left[\frac{(6.63 \times 10^{-34} \text{ J s})(3 \times 10^8 \text{ m/s})}{(1.5 \times 10^{-6} \text{ m})(1.38 \times 10^{-23} \frac{\text{J}}{\text{K}})(6050 \text{ K})}\right] - 1 \right\}^{-1},$$

$$L = 4.035 \times 10^{12} \text{ W/m}^3.$$

$$B_{\text{sqm-nm}} = d \frac{LR_s^2}{R_{es}^2} = 10 \text{ nm} \frac{(4.035 \times 10^{12} \text{ W/m}^3)(6.96 \times 10^8 \text{ m})^2}{(1.47 \times 10^{11} \text{ m})^2}$$

$$= 0.00905 \text{ W/m}^2$$

1-5. Calculate the MPE needed for a 1550-nm wavelength laser to be eye safe in the following configurations:

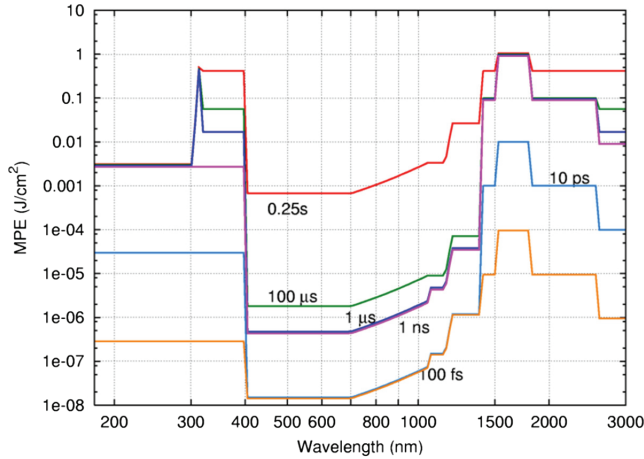
- At the exit aperture. The aperture is 1 square cm in area.
- At a spot 10 m from the aperture. The beam will spread to cover 20 deg in elevation and 3 deg in azimuth. The beam will scan back and forth in azimuth 10 times per second from the edge of the beam at 30-deg azimuth to the opposite edge of the beam at -30-deg azimuth.
- In the same geometry as (b), but with a laser wavelength of 900 nm.

For cases (a) through (c), assume 3-ns pulse widths.

1-5 Solution:

Our solution uses Fig. 1.11, which is repeated here. The plot shows that, for 1-ns pulses, the energy threshold is 1 J for 1550 nm and about 1×10^{-6} J for 900 nm. As stated in Section 1.7, Fig. 1.11 charts energy threshold per square cm for a 10-s exposure. For case (a), the exit aperture is 1 cm^2 ; therefore, we have an average power of 100 mW over 10 s to reach the 1-J/ cm^2 threshold. For case (b), the beam is 20 deg \times 3 deg and scans back and forth. Any given location is only illuminated a portion of the time. We actually can say that the

energy is spread over 20×60 deg. At 10 m away, this is an area of $3.49 \text{ m} \times 10.47 \text{ m}$, or 365,540 square cm. This is a lot of area. Our laser eye damage threshold is therefore very high: $3.65 \times 10^5 \text{ W}$. If we switch to 900 nm for the same case, the laser damage threshold is 0.365 W or 365 mW. This shows the significant impact of wavelength on MPE.



1-6. A monostatic direct-detection LiDAR uses a wavelength of 1550 nm.

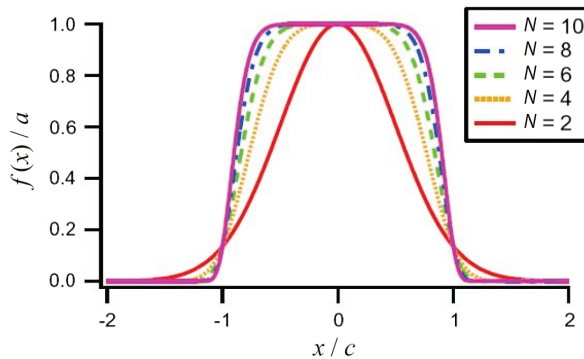
- Calculate the diameter of the transmit aperture for a divergence of less than 0.002 deg.
- Plot the radial intensity profile of the optical beam in orders of $N = 2, 4, 6, 8$ and 10.

1-6 Solution:

- Using Eq. (1.5), the aperture diameter is about 4.6 cm:

$$\theta = \frac{1.03\lambda}{D} \rightarrow D = \frac{1.03\lambda}{\theta} = \frac{1.03(1.55 \times 10^{-6} \text{ m})}{0.002 \text{ deg}(\pi/180 \text{ deg})} = 0.0457 \text{ m} = 4.57 \text{ cm}.$$

- The plot of the radial intensity profile for the optical beam in orders of $N = 2, 4, 6, 8$, and 10 is shown below:



1-7. What is the ratio of the separation in returns of the reflectivity between 14-bit and 8-bit digital returns for a uniform distribution of reflectivity between 9% and 12%?

1-7 Solution:

$$r = \frac{(0.12 - 0.09)}{2^8} = \frac{(0.12 - 0.09)}{256} = 0.0001719.$$

The LiDAR is required to discern a variation of 0.0001719 for 8 bits of grayscale.

$$r = \frac{(0.12 - 0.09)}{2^{14}} = \frac{(0.12 - 0.09)}{16384} = 1.8311 \times 10^{-6}.$$

The LiDAR is required to discern a variation of 1.8311×10^{-6} for 14 bits of grayscale.

Thus, the ratio of variation in reflectivities between a 14-bit and an 8-bit digital receiver is $0.0001719/1.8311 \times 10^{-6} = 0.01065$. The variation in reflectivity for a 14-bit receiver with a uniform distribution of reflectivity is 1.065% of that of an 8-bit receiver with the same distribution.

1-8. How many photons irradiate the entire surface of the earth from the sun at 540 nm? How much power arrives over a year?

1-8 Solution:

$$\lambda = 540 \text{ nm},$$

$$R_e = 6.96 \times 10^8 \text{ m},$$

$$R_{es} = 1.47 \times 10^{11} \text{ m},$$

$$R_e = 6.37 \times 10^6 \text{ m},$$

$$c = 3 \times 10^8 \text{ m/s},$$

$$h = 6.63 \times 10^{-34} \text{ J s}.$$

The number of photons per square meter on Earth's surface is given by

$$N = \frac{LR_s^2 \lambda}{R_{es}^2 hc}.$$

However, the total number of photons over Earth's surface is given by

$$n = NA = 4\pi R_e^2 N = 4\pi R_e^2 \frac{LR_s^2 \lambda}{R_{es}^2 hc}.$$

The blackbody radiation of the sun is given by

$$L = \frac{2hc^2}{\lambda^5} \left[\exp\left(\frac{hc}{\lambda kT}\right) - 1 \right]^{-1}$$

such that

$$\begin{aligned} n &= 4\pi R_e^2 \frac{LR_s^2\lambda}{R_{es}^2 hc} = 4\pi R_e^2 \frac{R_s^2\lambda}{R_{es}^2 hc} \frac{2hc^2}{\lambda^5} \left[\exp\left(\frac{hc}{\lambda kT}\right) - 1 \right]^{-1} \\ &= 8\pi R_e^2 \frac{R_s^2}{R_{es}^2} \frac{c}{\lambda^4} \left[\exp\left(\frac{hc}{\lambda kT}\right) - 1 \right]^{-1}, \\ n &= 8\pi R_e^2 \frac{R_s^2}{R_{es}^2} \frac{c}{\lambda^4} \left[\exp\left(\frac{hc}{\lambda kT}\right) - 1 \right]^{-1}, \\ n &= 8\pi (6.37 \times 10^6 \text{ m})^2 \frac{(6.96 \times 10^8 \text{ m})^2}{(1.47 \times 10^{11} \text{ m})^2} \frac{(3 \times 10^8 \text{ m/s})}{(5.40 \times 10^{-7} \text{ m})^4} \\ &\quad \left[\exp\left(\frac{(6.63 \times 10^{-34} \text{ Js})(3 \times 10^8 \text{ m/s})}{(5.40 \times 10^{-7} \text{ m})(1.38 \times 10^{-23} \text{ J/K})(6050 \text{ K})}\right) - 1 \right]^{-1}, \\ n &= 6.5664 \times 10^{45} \text{ photons m}^{-1}\text{s}^{-1}, \\ P &= nE_p d = nd \frac{hc}{\lambda} = (6.5664 \times 10^{45})(1 \times 10^{-9} \text{ m}) \\ &\quad \left[\frac{(6.63 \times 10^{-34} \text{ Js})(3 \times 10^8 \text{ m/s})}{(5.40 \times 10^{-7} \text{ m})} \right] = 2.419 \times 10^{18} \text{ W}. \end{aligned}$$

So, 2.419 million TW arrive each year from solar irradiation on the Earth's surface. Note that the actual value would be less by one-half (day versus night): 1.209 million TW annually over Earth's surface.

1-9. What distance would a 1-km² target need to be in order to be fully filled by laser illumination from an aperture of diameter 5 cm and wavelength of 1550 nm, assuming a diffraction-limited beam? Check to make sure you are in the far field.

1-9 Solution: The divergence is

$$\theta = \frac{1.03(1550 \text{ nm})}{5 \text{ cm}} = 31.9 \mu\text{rad}.$$

Thus, if we assume a circular target and a circular aperture/beam,

$$r_{\text{target}} = \frac{\sqrt{1 \text{ km}^2}}{\pi} = 318.3 \text{ m}.$$

The distance z traveled by the light path must equal the radius of the target divided by the tangent of the divergence angle:

$$z = \frac{r_{\text{target}}}{\tan \theta} = 9.969 \times 10^6 \text{ m} = 9969 \text{ km.}$$

Note that this is roughly between low Earth orbit and geostationary orbit as measured from a ground station. This also highlights an inherent problem in satellite characterization using active sources of illumination (LiDAR or radar) beyond low Earth orbit, i.e., at distances of a few hundreds of kilometers.

The far field is at

$$R = \frac{2D^2}{\lambda},$$

which means that the far field is 3.2 km away, so the target is in the far field.

1-10. Assume two lasers, both having a pulse width of 1 ns. One laser is 10-W average power, made up of a 10-kHz repetition rate with 1 mJ/pulse. The second laser has the same repetition rate but has only 10 μJ /pulse, so is a 100-mW average power laser. Both are at the 1550-nm wavelength. The first laser illuminates an area of 60 deg by 30 deg continuously in a flash LiDAR system. The second laser has a beam width of 1 deg but scans in azimuth over 60 deg. It also has an elevation coverage of 30 deg. The beam of the first laser is 60 deg wide by 30 deg high. The beam of the second laser is 1 deg wide by 30 deg high and has a scan rate of 1 Hz. For both lasers, calculate the flux (in W/cm^2) illuminating the eye at a range of 100 m, assuming that we are in the far field. Then compare each flux value against the eye-safety threshold.

1-10 Solution: For laser 1, we have 10-W average power, so the laser will emit 10 J in 10 s. The area covered is $A = 2 \times 100 \times \tan(30 \text{ deg}) \times 1 \times \tan(15 \text{ deg})$. This is 115 m by 58 m, or an area of 6188 m^2 . For laser 2, we have an area of 201 m^2 . Therefore, the flux is 1/6188 for laser 1, and 0.1/201 for laser 2 in W/m^2 . The flux in W/cm^2 is 1.6 for laser 1, and 5 for laser 2, but laser 2 is only illuminating the area for 1/60th of the time. Therefore, the total energy/ cm^2 in case 1 over 10 s is 16 J/cm^2 . For laser 2, it is 0.83 J/cm^2 . Laser 1 is not eye safe, even though it puts out more power. Laser 2 is eye safe. It is below the threshold of 1 J/cm^2 for 1550 nm.

References

1. Wikimedia Commons page on EM Spectrum. Adapted from File:EM Spectrum3-new.jpg by NASA. The butterfly icon is from the P icon set, P biology.svg. The humans are from the Pioneer plaque, Human.svg. The

- buildings are the Petronas towers and the Empire State Buildings, both from [Skyscrapercompare.svg](https://commons.wikimedia.org/w/index.php?curid=2974242). Released under license CC BY-SA 3.0, <https://commons.wikimedia.org/w/index.php?curid=2974242>.
2. National Academy of Sciences, *Laser Radar: Progress and Opportunities in Active Electro-Optical Sensing*, P. F. McManamon, Chair (Committee on Review of Advancements in Active Electro-Optical Systems to Avoid Technological Surprise Adverse to U.S. National Security), Study under Contract HHM402-10-D-0036-DO#10, National Academies Press, Washington, D.C. (2014).
 3. P. F. McManamon, *Field Guide to LiDAR*, SPIE Press, Bellingham, Washington (2015) [doi: 10.1117/3.2186106].
 4. Google Books Ngram Viewer: https://books.google.com/ngrams/graph?content=lidar%2Cladar&year_start=1960&year_end=2015&corpus=15&smoothing=3&share=&direct_url=t1%3B%2Clidar%3B%2Cc0%3B.t1%3B%2Cladar%3B%2Cc0.
 5. P. F. McManamon, T. A. Dorschner, D. L. Corkum, et al., “Optical phased array technology,” *Proc. IEEE* **84**(2), 268–298 (1996).
 6. P. F. McManamon, P. J. Bos, M. J. Escuti, et al., “A review of phased array steering for narrow-band electrooptical systems,” *Proc. IEEE* **97**(6), 1078–1096 (2009).
 7. V. Molebny, P. F. McManamon, O. Steinvall, T. Kobayashi, and W. Chen, “Laser radar: historical prospective—from the East to the West,” *Optical Engineering* **56**(3), 031220 (2016) [doi: 10.1117/1.OE.56.3.031220].
 8. P. F. McManamon, G. Kamerman, and M. Huffaker, “A history of laser radar in the United States,” *Proc. SPIE* **7684**, 76840T (2010) [doi: 10.1117/12.862562].